Image-guided phenotyping of ovariectomized mice : altered functional connectivity, cognition, myelination, and dopaminergic functionality

Image-guided phenotyping of ovariectomized mice: altered functional connectivity, cognition, myelination and dopaminergic functionality

Anckaerts Cynthia[a], van Gastel Jaana[b], Leysen Valerie[c], Hinz Rukun[a], Azmi Abdelkrim[b], Simoens Pascal[b], Shah Disha[a], Kara Firat[a], Langbeen An[d], Bols Peter[d], Laloux Charlotte[e], Prevot Vincent[c], Verhoye Marleen[a], Maudsley Stuart[b], Van der Linden Annemie[a]

[a]Bio-Imaging Lab, Department of Biomedical Sciences, University of Antwerp, Universiteitsplein 1, 2610 Wilrijk, Antwerp, Belgium;
[b]Translational Neurobiology Group, Department of Biomedical Science, University of Antwerp-VIB, Universiteitsplein 1, 2610 Wilrijk, Antwerp, Belgium;
[c]Development and Plasticity of the Neuroendocrine Brain, Inserm U1172, Jean-Pierre Aubert Research Centre, Labex Distalz, 1 place de Verdun, 59045 Lille cedex, France;
[d]Veterinary Physiology and Biochemistry, Department of Veterinary Sciences, University of Antwerp, Universiteitsplein 1, 2610 Wilrijk, Antwerp, Belgium;
[e]SFR DN2M, Inserm UMR-S1171/UMR-S1172, 1 place de Verdun, 59045 Lille cedex, France

Corresponding author
Cynthia Anckaerts
Email address: Cynthia.anckaerts@uantwerpen.be
Address: Bio-Imaging Lab, Department of Biomedical Sciences, University of Antwerp, Universiteitsplein 1, 2610 Wilrijk, Antwerp, Belgium
Phone number: +32 265 22 43

Abstract

A large proportion of the population suffers from endocrine disruption, *e.g.* menopausal women, which might result in accelerated aging and a higher risk for developing cognitive disorders. Therefore, it is crucial to fully understand the impact of such disruptions on the brain to identify potential therapeutic strategies. Here, we show using resting state functional MRI that ovariectomy and consequent hypothalamus-pituitary-gonadal (HPG) disruption results in the selective dysconnectivity of two discrete brain regions in mice. This effect coincided with cognitive deficits and an underlying pathological molecular phenotype involving an imbalance of neurodevelopmental/neurodegenerative signaling. Furthermore, this quantitative mass spectrometry proteomics-based analysis of molecular signaling patterns further identified a strong involvement of altered dopaminergic functionality (*e.g.* DAT and predicted upstream regulators DRD3, NR4A2), reproductive signaling (*e.g* Srd5a2), rotatin expression (rttn), cellular aging (*e.g.* Rxfp3, Git2), myelination and axogenesis (*e.g.* Nefl, Mag). With this, we have provided an improved understanding of the impact of HPG dysfunction and highlighted the potential of using a highly translational MRI technique for monitoring these effects on the brain.

Keywords

Functional connectivity, resting state fMRI, ovariectomy, cognition, behavior, quantitative proteomics, mass spectrometry, myelination, dopamine, aging

INTRODUCTION

Emerging research has demonstrated the involvement of the hypothalamic-pituitary-gonadal (HPG) axis in multiple non-reproductive processes, such as neurodevelopment, neuroplasticity and various brain functions including cognition. Because the HPG system has a regulatory role on many organs, including the brain, age-related degeneration of this system also seems implicated in aging and pathophysiology of certain cognitive disorders, *e.g.* Alzheimer's disease (AD) (Koebele and Bimonte-Nelson, 2017; Wang et al., 2010; Zarate et al., 2017). In line with this, numerous studies have reported an association between HPG-axis related hormones (*e.g.* estrogen) and neurogenesis, neuroprotection and cognition (For review, see *e.g.* (Arevalo et al., 2015; Blair et al., 2015; Brann et al., 2007; Hara et al., 2015; Vargas et al., 2016)). The trophic effect of sex steroid is critical in functions such as learning, memory, emotion, motivation, motor control and cognition (Horstink et al., 2003; Sacher et al., 2013; Sakaki and Mather, 2012; Sundstrom Poromaa and Gingnell, 2014; Toffoletto et al., 2014). An important mechanism through which these actions can be exerted is via interaction with different neurotransmitter systems (for review, see (Barth et al., 2015)). The link between reproductive axis hormones and cognition is further highlighted by expression of both GnRH and estrogen receptors in brain regions important for memory and cognition (Albertson et al., 2008; Hazell et al., 2009; Mitra et al., 2003; Shughrue et al., 1997; Wen et al., 2011), such as hippocampal and cortical regions.

As menopausal women are prone to cognitive decline and have a higher risk of developing AD (Vina and Lloret, 2010), research has focused on the role of decreased estrogens (Li et al., 2014) or elevated gonadotropins, particularly luteinizing hormone (LH) (Blair et al., 2015; Blair et al., 2016), in these pathological events. Evidence suggests that such a lack of sex hormones can lead to aberrant neurotransmission, mitochondrial dysfunction, a decline of synaptic plasticity, brain hypometabolism and an increase of neuroinflammation (Zarate et al., 2017). Although a putative causal link between this hormonal system and both normal and pathological brain functionality is evidenced by many studies, clinical studies investigating the potential beneficial effect of modulating the HPG-axis as a

therapeutic target in menopausal women have failed to provide an unequivocal conclusion as to its potential utility (Henderson, 2014; Rocca et al., 2011). Therefore, it is crucial to obtain a better basic comprehension of the impact of HPG functionality on the brain as this knowledge could potentially be exploited to prevent the etiological development of cognitive disorders or help create new remedial drug strategies.

Ovariectomized (OVX) animals offer an experimental platform to study the impact of HPG dysfunction on the brain in a controlled manner (Koebele and Bimonte-Nelson, 2016). Surgical removal of ovaries, *i.e.* ovariectomy, will cause a sudden decrease of estrogen production hence disturbing the entire HPG system. More specifically, due to the loss of negative feedback by estrogen, gonadotropin concentrations (luteinizing hormone, LH; follicle stimulating hormone, FSH) will increase, similar to the situation in natural or surgical menopause in women where loss of ovarian function has been linked to increased risk of various disorder such as Parkinson's or Alzheimer's disease, depression and anxiety (Parker et al., 2009; Rocca et al., 2008a; Rocca et al., 2016; Rocca et al., 2017; Rocca et al., 2008b; Rocca et al., 2011). A disturbance of the balance within this hormonal system can lead to various effects in both human and rodents, including decreased neuroplasticity, loss of neuroprotective cellular signaling modalities and neurotransmission deficits (Barth et al., 2015; Bosse and DiPaolo, 1996; Hara et al., 2015; Zarate et al., 2017). Furthermore, HPG dysfunction seems also linked to impaired cognitive function both in human and animal studies (Heikkinen et al., 2004; Iivonen et al., 2006; Toffoletto et al., 2014). However, interpreting this research is complicated due to the highly heterogeneous circumstances, *e.g.* differences in timing and duration of endocrine disruption as well as the type of potential hormone treatment. Despite some contradictory findings, the majority of current evidence points towards a significant effect of HPG-associated hormones on neural circuits implicated in cognition.

To examine neural circuits, resting state fMRI (rsfMRI) has proven to be a valuable technique. This is a non-invasive *in vivo* tool capable of monitoring whole-brain functional connectivity (FC) based on the fact that low frequency fluctuations (LFF, 0.01-0.1Hz) of the blood oxygenation level dependent

(BOLD) contrast can be detected when a subject is at rest. This phenomenon of FC is defined as the temporal dependency of neuronal activation patterns of anatomically separated brain regions and can be calculated by correlating measures of the LFFs of the BOLD signal (van den Heuvel and Hulshoff Pol, 2010). It has been suggested that ovarian hormones could enhance both cortico-cortical and subcortico-cortical functional connectivity, whereas androgens (testosterone) might decrease subcortico-cortical functional connectivity but increase functional connectivity between subcortical brain areas (For review, see (Peper et al., 2011)). Only few human studies examined resting state functional networks in (post)menopausal women or during the menstrual cycle showing either no changes (De Bondt et al., 2015; Hjelmervik et al., 2014) or FC alterations in brain regions such as the hippocampus and the frontal cortex (Comasco and Sundstrom-Poromaa, 2015; Huang et al., 2015; Lisofsky et al., 2015; Vega et al., 2016). Therefore, results concerning possible endocrine-driven functional alterations remain scarce and inconsistent. Going further on the idea that endocrine disruption could result in accelerated ageing, long-range connections are of particular interest as it has been shown that these are most vulnerable to disintegrate during ageing or disease processes (Dennis and Thompson, 2013; Fair et al., 2009; Tomasi and Volkow, 2012). For example, anterior-posterior connectivity, *i.e.* the functional connectivity between anterior brain regions (frontal cortex) and posterior brain regions (posterior cingulate/retrosplenial cortex, medial temporal regions), has been shown to be high in young adults and to decrease during ageing. Furthermore, the strength of this connection has been linked to cognitive performance as well (Andrews-Hanna et al., 2007; Vidal-Pineiro et al., 2014).

The present study was devised to examine whether a disturbance of the HPG-axis can affect intrinsic functional brain networks in mice, reflecting an accelerated aging phenotype. For this purpose, mice were either ovariectomized or sham-operated at the onset of adulthood (age of three months). The intrinsic FC of the brain was monitored monthly using rsfMRI until the age of seven months to evaluate whether altered patterns of FC could be identified after ovariectomy. Based on the rsfMRI outcome, complementary behavioral tests were performed in a separate cohort of seven month old mice to

investigate whether FC deficits coincided with cognitive impairment. Lastly, a quantitative mass spectrometry proteomics-based analysis of molecular signaling patterns was employed to unravel the signaling mechanisms underlying the observed rsfMRI alterations in affected brain regions of seven month old OVX mice.

MATERIAL AND METHODS

Ethical statement

All procedures were performed in strict accordance with the European Directive 2010/63/EU on the protection of animals used for scientific purposes. The research protocols employed were approved by the Committee on Animal Care and Use at the University of Antwerp, Belgium (permit number 2014-56) and all efforts were made to minimize animal suffering.

Animals

C57BL/6J mice (12 weeks old, female, N=36) were used throughout the MRI study (Jax mice strains, Charles River Laboratories). One week after a baseline rsfMRI scan at three months of age, *i.e.* the onset of adulthood, mice were randomly divided into two groups: an ovariectomized group (OVX, N=18) and a sham-operated group (Sham, N=18). After the surgical procedure, the diet was changed to a low phytoestrogen diet (Sniff R/M-H, www.ssniff.de, Germany). Mice were assessed monthly using rsfMRI between the ages of three and seven months. Due to poor data quality (*e.g.* excessive movement or whole-brain unspecific FC) several scans were excluded, resulting in effective group sizes of 15-17 Sham mice and 13-18 OVX mice across the time points investigated (OVX: N_{3M}=13, N_{4M}=18, N_{5M}=16, N_{6M}=16, N_{7M}=14; Sham: N_{3M}=16, N_{4M}=16, N_{5M}=17, N_{6M}=16, N_{7M}=15). Behavioral analyses were performed in a separate cohort of seven month old mice (N_{OVX}=12; N_{Sham}=11) to avoid any confounding effect of repeated scanning/anesthesia on the behavioral outcome. From this group, brain tissue samples were collected for *ex vivo* analyses as described below. The selection of brain regions for further *ex vivo* analyses was guided by the rsfMRI readout.

Surgical procedure: ovariectomy

Prior to surgery, the weight of each animal was measured with a digital balance. Animals were anesthetized using an intraperitoneal injection of Anesketin® (80-100 mg ketamine/kg BW) / Rompun® (10 mg xylazine/kg BW) / Temgesic® (0.1 mg buprenorphine/kg BW). Fur on the mouse abdomen was removed and a small abdominal incision caudal of the umbiculus was made. After the peritoneal cavity was accessed, both left and right uterine tubes and ovaries were identified. Next, the distal part of both uterine horns, ovaries and surrounding fat were removed by ligation using Vicryl suture 6-0 sutures for the OVX group. After removal of the ovaries, the abdominal cavity was closed (continuous sutures for the abdominal muscles; separate sutures for closing of the skin). The Sham group received a similar protocol where the abdominal cavity was accessed and then closed again, without removing any tissue nor ligating any structures. After the surgical procedure, mice were allowed to recover in a heated cage and were observed until full recovery (Langbeen et al., 2016).

Plasma LH concentration

To ensure that the ovariectomy was successful in both cohorts of mice, the expected cessation of the estrus cycle was monitored by cytological examination of vaginal smears. Because OVX female mice showed constant estrus, plasma levels of the luteinizing hormone (LH) were measured in blood samples also collected in estrus in Sham mice, which were previously exposed to male urine via soiled bedding to synchronize their estrus cycles (Ryan and Schwartz, 1980; Whitten, 1956). LH was assayed using a protocol previously described by others (Messina et al., 2016; Steyn et al., 2013). A detailed description of the LH assay procedures can be found in SI Material and Methods.

Resting state functional MRI procedure

For MRI procedures, mice were initially anesthetized with 2% isoflurane (IsoFlo, Abbott, Illinois, USA), which was administered in a mixture of 70% nitrogen (400 cc/min) and 30% oxygen (200 cc/min). During rsfMRI acquisitions, a combination of isoflurane (0.4%) and medetomidine (0.3 mg/kg; Domitor, Pfizer, Karlsruhe, Germany) was used to sedate the animals as previously described (Shah et al., 2016a; Shah et al., 2016b). Briefly, mice received a subcutaneous (s.c.) bolus of medetomidine after which the isoflurane was reduced to 1%. Five minutes before the rsfMRI acquisition, isoflurane

was further decreased to 0.4%. The rsfMRI acquisition was started 40 minutes after bolus injection while keeping the isoflurane level constant at 0.4%. After imaging procedures were performed, the effects of medetomidine were counteracted by the s.c. injection of 0.1mg/kg atipamezole (Antisedan, Pfizer, Karlsruhe, Germany). The physiological status of the animals was monitored throughout the imaging procedure. A pressure sensitive pad (MR-compatible Small Animal Monitoring and Gating system, SA Instruments, Inc.) was used to monitor breathing rate and a rectal thermistor with feedback controlled warm air circuitry (MR-compatible Small Animal Heating System, SA Instruments, Inc.) was used to maintain body temperature at (37.0 ± 0.5) °C.

MRI procedures were performed on a 9.4T Biospec MRI system (Bruker BioSpin, Germany) with Paravision 5.1 software. Images were acquired using a standard Bruker cross coil set-up with a quadrature volume coil and a quadrature surface coil for mouse brain. Three orthogonal multi-slice Turbo RARE T2-weighted images were acquired to render slice-positioning uniform (repetition time 2000 ms, echo time 15 ms, 16 slices of 0.4 mm). Field maps were acquired for each animal to assess field homogeneity, followed by local shimming, which corrects for the measured inhomogeneity in a rectangular volume of interest within the brain.

Resting-state signals were measured using a T2*-weighted single shot echo-planar-imaging (EPI) sequence (repetition time 2000 ms, echo time 15 ms, 16 slices of 0.4 mm, slice gap 0.1mm, 150 repetitions) with a total scan time of 5 minutes. The field-of-view was (20x20) mm^2 and the matrix size (128 x 64), resulting in pixel dimensions of (0.156 x 0.312) mm^2.

Resting state data analysis

Pre-processing of the rsfMRI data was performed as described earlier (Jonckers et al., 2011). Realignment, normalization and smoothing was performed using SPM12 software (Statistical Parametric Mapping, http://www.fil.ion.ucl.ac.uk). First, all images within each session were realigned to the first image. This was performed using a least-squares approach and a 6-parameter (rigid body) spatial transformation. Second, all datasets were normalized to a study specific EPI template obtained by averaging all baseline scans. The normalization steps consist of a global 12-parameter affine

transformation followed by the estimation of the nonlinear deformations. Finally, in plane smoothing was performed using a Gaussian kernel with full width at half maximum of twice the voxel (0.31 x 0.62) mm^2 (Jonckers et al., 2011). Next, resting state data was filtered (0.01 – 0.1 Hz) using the Resting-State fMRI Data Analysis Toolkit (REST1.8) in Matlab 2014a to extract relevant data and rule out noise and low frequency drift. Due to poor quality or excessive movement, several scans had to be excluded, resulting in effective group sizes of 15-17 Sham mice and 13-18 OVX mice across the time points investigated.

Independent Component Analysis (ICA) was performed on the rsfMRI data of three months old animals, to determine which resting-state networks could be observed in healthy animals (Jonckers et al., 2011). ICA was performed using the GIFT-toolbox (Group ICA of fMRI toolbox version 2.0a: http://icatb.sourceforge.net/), by implementing spatial ICA which estimates sources as being statistically spatially independent. First, a two-step data reduction step is performed by principal component analysis, after which the data of each individual animal is concatenated. Then, group ICA was performed using the Infomax algorithm. The final step is back reconstruction of the data to single-subject independent components and time courses. ICA was performed using a pre-set of 15 components, which was shown to be appropriate to identify relevant resting-state networks in mice. Based on this analysis, the anterior/prefrontal and posterior/retrosplenial FC networks were identified and masks were created from the relevant ICA components.

Regions of four voxels each were indicated with the anatomically relevant ICA components and the Mouse Brain Atlas (Franklin, 2007) as reference in MRIcron software (http://www.mricro.com/mricron). For the anterior/prefrontal network, the following seeds were indicated: left and right anterior cingulate cortex (aCg) and prelimbic cortex (PrL). For the posterior/retrosplenial network, seeds were selected in the left and right retrosplenial cortex (Rs) and parietal association cortex (PaA). These seeds were then used to extract the respective temporal signal of each subject using Rest 1.8.

Anterior-posterior (A-P) connectivity was calculated in two different ways: (i) based on a ROI-based analysis or (ii) based on a seed-based analysis. Method (i) involved the computation of all pairwise correlations (z-values) between the rsfMRI time series of regions of the anterior network (aCg, PrL) and the posterior network (Rs, PaA) resulting in a matrix as shown in Fig. 2B. More specifically, for region of interest (ROI) based FC analysis, the BOLD time course of each seed region was extracted after which linear correlation between the selected time courses, *i.e.* a measure of the strength of FC between the respective ROIs, was calculated using a cross-correlation analysis in REST 1.8. A Fisher's z transform was performed on all correlation coefficients. The z-transformed correlation values were presented in a zFC matrix, with a threshold to exclude z-values below 0.05 ($|z|<0.05$) (Shah et al., 2016c). Next, these individual pairwise FC values were classified according to the anterior or posterior network and were used for further between-network FC computations, *i.e.* the average of all pairwise correlations between anterior and posterior regions. Method (ii), based on a seed based analysis of the Rs cortex, involved the computation of individual statistical FC maps. Briefly, the extracted temporal signal of the Rs seed was compared to all other voxels of the brain using a linear model in SPM12, resulting in individual FC maps containing all voxels significantly correlated with the given temporal signal. Next, individual t-values were extracted for each subject within the restrictions of the anterior network (ICA component) mask. Additionally, individual cluster sizes were extracted from the subject's statistical FC maps within the restrictions of the relevant ICA component masks.

Behavioral assessments

To evaluate whether FC changes as observed by rsfMRI at the age of seven months coincided with behavioral deficits, a separate cohort of seven month old Sham and OVX mice was subjected to a series of behavioral tests. Similar to the first cohort, these mice were ovariectomized or sham-operated four months prior to testing, *i.e.* at the age of three months. Behavioral tests were specifically selected based on the regions affected according to the rsfMRI outcome and included the spontaneous alternation (SA) test, novel object recognition (NOR) test, Barnes maze and passive avoidance (PA) test.

Y-maze spontaneous alternation test

The spontaneous alternation test (Hughes, 2004) was used to assess working memory of rodents in a Y-maze (3 arms of 8x30 cm), which requires proper function of hippocampal and frontal brain regions (Lalonde, 2002). Furthermore, it has been shown that working memory can bemodulated by ageing and hormonal status (Cao et al., 2013; Lalonde, 2002). This test is based on the fact that mice will show the tendency to explore the different arms with alternation of arms visits rather than returning to the previous arm. Mice were placed in one of the arm (randomized between subjects) and allowed to explore the entire maze for 8 minutes. Every entry to an arm was recorded and defined as entering the arm with all four paws. Performance of mice in this test was calculated as percentage alternation, defined as the ratio of the number of triads (entering each of the three arms consecutively) over the total number of arm entries.

Novel object recognition test

The novel object recognition (NOR) test was used to assess recognition memory, involving frontal and parietal association cortices (Leger et al., 2013). Interestingly, Fonesca and Bastos and colleagues previously reported impairments in NOR after ovariectomy, which could be recovered by hormone replacement therapy (Bastos et al., 2015; Fonseca et al., 2013). The NOR consisted of an initial habituation day in which the mice were placed in an empty arena (50x50 cm) for 10 minutes to acclimatize to the novel environment. The following day, two identical objects (pair A) were placed on opposite sides in the cage. During the object exploration training, the mouse was placed in the arena and was allowed to explore the objects for 15 minutes. On the test day, 24 hours later, the animals were placed in the arena for 15 minutes, which contained two identical objects (pair B, different than the previous day). One hour later, the mouse was again placed into the arena for 5 minutes, which now contained one familiar object (of pair B) and one completely new object. To assess the recognition memory function, the discrimination index was calculated as the ratio of the time spent exploring the new object over the total objects exploration time.

Barnes maze

The Barnes maze was used for measuring visuo-spatial learning and memory (Sunyer et al., 2007). By altering the specific set-up of this test, both learning and long-term memory can be evaluated. Spatial memory is dependent on various brain regions, including the hippocampus, parietal cortex, entorhinal cortex, prefrontal and retrosplenial cortex. Importantly, the learning phase of this test is highly dependent on hippocampal function, whereas the later memory retention phase strongly relies on cortical integration (Bontempi et al., 1999; Izquierdo and Medina, 1997; Maviel et al., 2004; Miller, 2000; Todd and Bucci, 2015). Alterations in spatial memory and retention have been reported previously after hormonal modulations (Ping et al., 2008; Sandstrom and Williams, 2001; Sarkaki et al., 2008).

The Barnes maze consisted of a circular platform (120 cm of diameter) with 40 equally spaced holes, of which one target hole gave entrance to a dark target box. The maze was surrounded by visual cues of different colors and shapes. The test consisted of an initial 4 training days and 1 test day (day 5). For each trial, the animal was placed onto the middle of the maze in an opaque cylindrical tube to ensure an initial disorientation before starting. Each trial is initiated by removing the opaque cylinder. On the first day, the mouse was allowed to explore and guided to its respective escape hole and left inside for one minute. Next, the training consisted of 4 days with 4 trials of 3 minutes per mouse (15 minutes in between every trial). The same target hole was used for one subject along all the training, with a different target hole between subjects. On day 5, the first test day, no escape box was placed and the animal was allowed to explore the platform for 90 seconds. This final test was repeated one and two weeks after training, on day 12 and 19 respectively, to assess the long-term retention ability of mice (Sunyer et al., 2007). Primary errors were assessed by counting the number of wrong escape holes a subject explored before finding the correct target hole. Primary latency was calculated, *i.e.* the time it took for a subject to find the target hole. In case a subject was not successful, this time was set at 90 seconds as a cut-off time. Lastly, the time spent in the target area was assessed as subjects should show a preference for this area of the maze.

Passive avoidance test

The passive avoidance test was used to evaluate aversive learning, which involves various brain regions such as the prefrontal cortex and amygdala. Especially the cholinergic system has been linked to performance in this test and impaired performance has further been observed after ovariectomy (Das et al., 2002). Passive avoidance learning was tested in a step-through box (Marciniak et al., 2015). The step-through box consisted of an aversive brightly lit compartment connected with a dark compartment by means of a sliding door. Mice were placed in the illuminated compartment during 90 seconds at maximum, and after 5 seconds the sliding door connecting both compartments was opened. Upon complete entry into the dark compartment (4-paw criterion), animals received a slight foot shock (0.2 mA, 2 s). Exactly 24 h later, mice are placed once again in the illuminated compartment and the escape latency to re-enter the dark compartment was timed up to 300 seconds.

Mass spectrometry and quantitative proteomics of murine cortex samples

To elucidate the molecular signaling pathways responsible for the OVX-induced alterations of FC and cognition, an unbiased quantitative proteomic approach using iTRAQ (isobaric mass-tag labelling for relative and absolute quantitation) mass spectrometry was applied to simultaneously identify and quantify the proteins that are differentially up- or down-regulated in fresh frozen murine cortical samples of OVX or Sham mice. Based on the outcome of the rsfMRI analysis, prefrontal (Pf) and retrosplenial (Rs) cortex samples were collected from mice previously subjected to the behavioral assessments (average age: 7,7 months; N_{Sham}=4; N_{OVX}=4) and processed as described in detail in SI Material and Methods.

Briefly, the raw data were analyzed by Proteome Discoverer 2.0 Software (ThermoScientific) using Sequest HT as search engine against the human UniProt/SwissProt database with threshold of confidence above 99% (false discovery rate (FDR) < 1%). The list of identified proteins, containing iTRAQ ratios of expression levels over control (Sham) samples, was generated. Proteins identified according to the statistical MS cut-offs were then subsequently used for further bioinformatics analyses. To identify the significantly altered proteins, *i.e.* proteins differentially expressed due to OVX surgical intervention exposure compared to sham surgery exposure, raw iTRAQ ratios (OVX:sham)

were first log_2 transformed. Following log_2 ratio transformation differentially expressed protein (DEP) lists were created by identifying only proteins that possessed log_2-transformed iTRAQ ratios two standard deviations ($p<0.05$) from the calculated mean background expression variation level. These results were further verified with western blots.

Significant DEP lists (comprising proteins elevated or reduced in their expression in cortex tissue samples in response to OVX surgical intervention) were then employed for further bioinformatics deconvolution using diverse informatics platforms including Ingenuity Pathway Analysis (IPA) (Canonical Signaling Pathway and Upstream Regulator applications; https://www.qiagenbioinformatics.com/products/ingenuity-pathway-analysis/), VennPlex ((Cai et al., 2013); https://www.irp.nia.nih.gov/bioinformatics/vennplex.html) and Network Analyst (http://www.networkanalyst.ca/).

Finally, a targeted natural language processing (NLP) investigation was performed to identify the specific functional intersection between steroid-related activity (implementation of ovariectomy) and the DEP datasets from both cortical samples. To this end, using the latent semantic indexing platform GeneIndexer, the specific DEPs from either dataset could be associated with our user-defined concept terms related to estrogenic activity in the brain. GeneIndexer is able to identify the strongest concept (user-defined input word) and term (Gene Symbol) correlation scores for any given input dataset using gene-word document analysis of over 20 million curated PubMed abstracts (Cashion et al., 2013; Chen et al., 2013). Here, we used the word concepts *menopause, aging, ovariectomy, estrogen/oestrogen, estradiol/oestradiol* and *estrogen receptor/oestrogen receptor* to identify the most strongly associated proteins across all of these terms from both Pf and Rs cortex DEP datasets. To simplify the numerical analysis of this output the following synonymous term Cosine similarity scores were summed together to create a comprehensive score, *i.e*. scores for '*estrogen*', '*oestrogen*', '*estradiol*', '*oestradiol*' were summed together and scores for '*estrogen receptor*' and '*oestrogen receptor*' were summed also.

Through ranking of the top 20 strongest correlating proteins (via both sum and mean of the Cosine Similarity scores across all the input concepts) a prioritized key group of proteins for each DEP list was

created. Using *Enrichr*-based (http://amp.pharm.mssm.edu/Enrichr/) interrogation of ligand-induced Gene Expression Omnibus (GEO) dataset alterations (https://www.ncbi.nlm.nih.gov/geo/) lists of strongly-correlating Ligand-controlled curated GEO response datasets were generated for the Rs and Pf cortex input datasets (20 proteins). We next extracted the specific words describing the significantly-associated ($p<0.05$) ligand-controlled GEO datasets and then created frequency-dependent wordclouds from these ligand terms. Next, these proteins were cross-interrogated with a functional disease database (also via Enrichr), *i.e.* the JENSEN Disease database (https://diseases.jensenlab.org/) to identify possible related disorders.

Statistical analyses

Statistical analyses of the physiological parameters, functional connectivity data as well as the behavioural data were performed using a linear mixed model analysis in JMP Pro 13 software with group and age as fixed effects and subject as random effect. In case no significant interaction effect [age x group] was found, only main effects (group or age) are reported. *Post hoc* tests were performed using the Tukey HSD (honest significance difference) multiple comparison test with $p<0.05$. To explore the A-P FC pattern in both groups in more detail, an additional hypothesis-driven analysis of group-specific ageing effects was performed by performing a mixed model analysis split by group (*i.e.* explore the age effect within each group separately). Finally, to evaluate the relation between age and A-P FC strength, a linear regression analysis was performed. To evaluate whether the outcome of this linear regression differed significantly between both groups, a one-way analysis of covariance (ANCOVA) was performed to evaluate the effect of age on A-P FC with group (OVX or Sham) as covariate.

Group-wise average seed-based FC maps were computed in SPM12 software using a one-sample T-test (unc. $p<0.001$; minimum cluster size $k>10$; (Shah et al., 2018)). The extracted t-values or z-values as well as cluster sizes were examined using two-sample t-tests. In case of multiple t-tests in parallel, a Holm-Sidak correction for multiple comparisons was applied ($p<0.05$).

Results obtained from the western blots were examined using unpaired t-tests to evaluate whether expression of the specific proteins differed significantly between OVX and Sham mice.

All reported values are shown as mean ± standard error.

RESULTS

Increased body weight and plasma LH after ovariectomy

An analysis of body weight and plasma LH of OVX and Sham mice revealed a significant [age x group] interaction effect ($F_{4,136}$=6.478, p<0.0001; Fig. 1). Whereas both groups gained a significant amount of weight during the experiment, a clear distinction was present between both groups. As such, the OVX group ranged from (21.28 ± 0.18) g at three months to (27.44 ± 0.72) g at seven months, while the Sham group only ranged from (21.5 ± 0.22) g at three months to (25.06 ± 0.26) g at seven months. According to the *post hoc* analysis, only the OVX group gained a significant amount of body weight one month after the surgery, *i.e.* at four months of age (3M vs. 4M: p_{OVX}<0.0001; p_{Sham}=0.2303). In contrast, Sham mice gained weight at a slower rate as compared to the OVX (3M vs. 5M: p_{OVX}<0.0001; p_{Sham}<0.0001). This difference in body weight between both groups became significantly different starting at the age of six months, *i.e.* three months after OVX (OVX vs. Sham: p_{6M}=0.0438; p_{7M}=0.0209). In order to confirm the success of the ovariectomy, plasma LH concentrations were examined. A significant [age x group] interaction was found ($F_{2,37}$=31.63; p<0.0001; Fig. 1), with significantly increased LH concentrations in the OVX group one month after the OVX intervention (p<0.0001 for all comparisons with three months), whereas no change was present in the Sham group. No difference in plasma LH was present at the baseline pre-surgery time point (OVX vs. Sham p_{3M}>0.99), however, at every time point after OVX intervention, LH concentrations were significantly higher in the OVX group compared to the Sham group (p<0.0001 for all group comparisons after three months).

Anterior-posterior brain functional connectivity is attenuated by ovariectomy

An initial analysis of the baseline rsfMRI data indicated no differences between 3 month old mice which were afterwards randomly divided into the OVX or Sham group. Next, an independent component analysis (ICA) of the rsfMRI data at baseline conditions discerned several FC networks similar to previously described mouse rsfMRI networks (Fig. S1) (Jonckers et al., 2011; Shah et al., 2016a; Zerbi et al., 2015). These included the functional anterior/prefrontal (Pf) and posterior/retrosplenial (Rs) networks, which were used for further anterior-posterior (A-P) FC calculations (Fig. 2A) as it has been shown that these long-range connections are especially vulnerable to aging (Damoiseaux et al., 2008; Vidal-Pineiro et al., 2014). With reference to these networks, regions-of-interest (ROIs) were defined to compute z-transformed FC matrices (Fig. 2B) from which FC between regions in the Pf and Rs network, *i.e.* A-P FC, was calculated (Fig. 2C).

Here, a significant group effect ($F_{4,32}$=4.93; p=0.0337) revealed that A-P FC in OVX mice was significantly lower compared to Sham mice. It can be appreciated from Fig. 2C that this effect was most pronounced at 7 months of age. A further hypothesis-driven analysis of potential group-specific ageing effects revealed that only in the Sham group a significant age-dependent strengthening of A-P FC could be observed (Sham: $F_{4,60}$=3.72; p=0.0091; OVX: $F_{4,61}$=0.70; p>0.05). More specifically, whereas A-P FC in OVX mice remained low and similar to baseline values throughout the study, Sham mice displayed an age-dependent strengthening of this connection when comparing baseline values at 3 months with A-P FC at the age of 6 (Sham 3M vs. 6M: p=0.0104) and 7 months (Sham 3M vs. 7M: p=0.0164). A linear regression analysis (Fig. 2D) further confirmed that a significant positive correlation between A-P FC and age was only present in Sham mice (Sham: R^2=0.1369, p=0.0007; OVX: R^2=0.006, p>0.05) and that this evolution differed significantly from the OVX group ($F_{1,154}$=6.057, p=0.0150).

Next, a seed-based analysis of the left Rs region, *i.e.* the main seed for the posterior network, was performed to confirm the observed differences in A-P connectivity at the age of seven months (Fig. 2E-F). From the individual FC maps, t-values and cluster size were extracted within the restrictions of the respective ICA component masks. Lower T-values were present in the anterior brain areas for seven month old OVX mice (p=0.0097; Fig. 2F), indicating a reduced strength of FC between anterior

411 regions and the Rs seed compared to age-matched sham mice. Additionally, a smaller cluster size in
412 both anterior and posterior regions ($p_{posterior}$=0.045; $p_{anterior}$=0.011) was present in the OVX mice,
413 indicating a lower extent of FC with the Rs seed (Fig. 2F).
414
415 **Cognitive impairments four months after ovariectomy**
416 Based on the rsfMRI outcome, a set of behavioral tests tailored to assess the function of the Pf and Rs
417 brain regions was selected to evaluate whether cognitive deficits were present alongside the FC
418 alterations four months after ovariectomy. This selection of behavioral tests was further based on
419 previous literature showing that performance in these tests can be modulated by hormonal
420 alterations, as described previously in the respective 'Material and Methods' sections.
421 The passive avoidance (PA) test revealed a significant [test day x group] interaction effect ($F_{1,19}$=5.17;
422 p=0.0348). *Post hoc* tests revealed that OVX mice did not present an increased latency to enter the
423 dark compartment on the test day. In contrast, Sham mice had a significantly increased retention
424 latency on the test day compared to the training day (Sham test day vs. Sham training day: p=0.0057)
425 and this latency was significantly longer than OVX mice at the test day (Test day Sham vs. OVX:
426 p=0.0271). These results indicate an impaired PA retention ability for the OVX group (Fig. 3A).
427
428 The Barnes maze test indicated that long-term spatial memory deficits were present in OVX mice (Fig.
429 2B-E). More specifically, OVX mice were able to learn the target spatial position as fast as Sham mice
430 during training (data not shown). However, a marked smaller proportion of OVX mice presented a
431 reduced retention ability during the single trial tests at 1 (day 5), 7 (day 12) and 14 days (day 19) after
432 training. As such, only half of the OVX group successfully accomplishing this trial at day 19, two weeks
433 after training (Fig. 3B). Compared to Sham mice, OVX mice made more primary errors ($F_{1,21}$=15.06;
434 p=0.0009) with the most pronounced difference occurring on day 19 (Fig. 3C). Also, OVX mice had a
435 consistently longer primary latency compared to Sham mice, indicating that they found their target
436 hole slower ($F_{1,21}$=5.99; p=0.0233; Fig. 3D). Furthermore, OVX mice spent less time in the target zone

compared to Sham mice ($F_{1,21}$=4.86; p=0.0388). It can be appreciated from Fig. 3E that this difference was most pronounced at day 19, *i.e.* two weeks after training.

The spontaneous alternation test, which assesses working memory dependent on hippocampal and frontal brain regions (Lalonde, 2002), did not reveal differences between both groups. Likewise, no differences were found for the novel object recognition test which evaluates associative memory involving frontal and parietal association cortical regions (data not shown).

Molecular signaling alterations four months after ovariectomy

Based on the MRI outcome, Pf and Rs cortical samples were acquired from seven month old OVX and Sham mice to explore the underlying molecular signaling alterations. Using stringent and significant cut-off criteria for protein identification (99% percentile identification confidence) and significant deviation from the expression background (95% percentile deviation from control levels) we found that long-term HPG dysfunction, *i.e.* four months after OVX, resulted in the significant alteration of multiple cortical proteins (Fig. S2A): Pf cortex - 162 (140 upregulated, 22 downregulated; Table S1); Rs cortex - 230 (169 upregulated, 61 downregulated; Table S2).

Canonical signaling pathway analysis

Quantitative proteomics is able to sample protein expression patterns at a mass level and is therefore able to, with effective bioinformatic interpretation, infer complex signaling behavior based on the co-expression of hundreds of proteins (Maudsley et al., 2011). Using these differentially expressed protein (DEP) profiles as inputs into Ingenuity Pathway Analysis (IPA), we identified 17 and 15 significantly-populated canonical signaling pathways respectively (Fig. S2B). Using a comparative hierarchical clustering of the significantly-populated signaling pathways between the two cortex sources we found that among the most highly-enriched signaling pathways was the '*Dopamine Receptor Signaling*' pathway (including proteins DAT or SLC6A3, dopamine transporter and DARPP32 or Ppp1r1b, Dopamine- and cAMP-regulated neuronal phosphoprotein). With respect to the distinctions between the two tissue sources it was apparent that developmentally-associated signaling pathways (*e.g.* '*TGF-beta signaling*', '*Epithelial Adherents Junction signaling*', '*Osteoarthritis*

signaling') were prominent in the Rs cortex while pathways associated with neurotrophic and reproductive signaling (*e.g*. '*CREB signaling in neurons*', '*CDK5 signaling'*, '*Relaxin signaling'*) were prominent in the Pf samples.

Upstream functionality analysis

Next, we sought to identify potential protein/ligand-based factors whose perturbation may result in the generation of the DEP patterns we observed. These analyses in both cortical regions again predicted multiple dopamine-related factors that generate molecular signature alterations reminiscent of our DEP datasets from the two cortical samples (*e.g*. DRD3 - dopamine receptor D3; NR4A2 - nuclear receptor subfamily 4, group A, member 2 (Montarolo et al., 2016; Reuter et al., 2017); Fig. 4A). We also found a clear distinction between the two regions with mainly altered neurodegenerative factors in the Rs cortex, while the Pf DEP patterns were more related to neurodevelopmental factors. A potential factor linking these two disparate events is likely to be the functionality of dopaminergic neural circuits that may facilitate this trans-cortex communication.

Western blot

Western blots were employed to verify our findings. We first confirmed that OVX intervention resulted in the significant upregulation of both rotatin (Rttn; p=0.0297, n=4) and syntaxin-4 (Stx4; p=0.0128, n=4) in the prefrontal cortex (Fig. S2C). Next, we confirmed the significant downregulation of the relaxin-3 receptor (Rxfp3) in the Rs cortex after OVX (p=0.0013, n=4; Fig. S2D), supporting the bioinformatic analysis which revealed a stronger representation of 'Relaxin signaling' in the Pf cortex as opposed to the Rs cortex (Fig. S2B). It has been proposed that Rxfp3 receptor forms a close functional link (van Gastel et al., 2016) with the neurometabolic aging regulator, Git2 (G protein-coupled receptor kinase interacting protein 2; (Chadwick et al., 2012; Lu et al., 2015; Martin et al., 2015; Siddiqui et al., 2017)). With respect to this association we found that alterations of cortical Git2 expression mirrored that of Rxfp3 (reduction in expression, p = 0.0001, n=4), thus further reinforcing the posit that OVX induces an accelerated ageing phenotype as genomic deletion of Git2 is associated with accelerated aging and cellular senescence (Chadwick et al., 2012; Lu et al., 2015; Siddiqui et al., 2017).

Network-based deconvolution of the coherently-regulated protein signatures

We next performed a more in-depth investigation into the interactive nature of the 31 proteins coherently regulated using a network topology-based approach. We identified six distinct functional subnetworks (SNs) of functionally-associating proteins (Fig. 4B). The two largest SNs - SN1 and SN2 – were both found to be associated with '*Axogenesis*'. Using a standard network graph annotation system (*i.e.* degree and betweenness ('centrality')) SN1 was centered around *Nefl* (Neurofilament light polypeptide) a protein strongly associated with '*Neuronal structural regulation*', whereas SN2 was centered upon the neuronal transmission-regulator *Mag* (Myelin-associated glycoprotein). SNs 3 and 4 were associated with '*Cell Cycle activity*' (centered upon *Sirt2* - NAD-dependent protein deacetylase sirtuin-2) and '*Reproductive functionality*' (centered upon *Cldn11* – Claudin 11) respectively. SNs 5 and 6 demonstrated a coherence of function as SN5 was linked to '*Neuronal transmission/apoptosis*' (centered upon *Ache* – Acetylcholinesterase) while SN6 was strongly linked to '*Dopaminergic neurotransmission and secretion'* (centered upon *Slc6a3* - Sodium-dependent dopamine transporter).

Targeted natural language processing (NLP) investigation of the DEP datasets

Finally, we identified the specific functional intersection between our own user-defined '*concept'* terms related to estrogenic activity in the brain and the DEP datasets from both cortical samples using a targeted natural language processing (NLP) approach. As our experimental paradigm involved the direct implementation, via ovariectomy, of dramatic alterations in gonadal steroids we next adopted an informatics approach to identify the specific functional intersection between steroid-related activity and our DEP datasets from both Prefrontal (Pf) or Retrosplenial (Rs) cortex samples. For the two input DEP lists the total cumulative Cosine similarity scores for all the proteins demonstrating at least an implicit association (*i.e.* Cosine Similarity score > 0.1) with each of the denoted concept terms related to estrogenic activity in the brain is indicated in Fig. 4C. For each protein-term score combination the number of proteins identified showing an implicit textual association with our user-defined concept (*e.g.* 'menopause') is identified above the column. In addition, the highest Cosine Similarity-scoring protein from each sample against any of the specific concepts is indicated. For the

majority, *i.e*. 4/5, both the number and degree of textual correlation to the specific concept was greater with the Rs compared to the Pf cortex dataset DEPs. This perhaps suggests that the proteomic alterations here were most profoundly affected, compared to the Pf cortex samples, by disruption to estrogenic functionality. This also correlates to the more 'pathological' alteration of signaling pathways and also reproductive signaling systems (*e.g*. the RXFP3 receptor) observed with our pathway analysis of Rs cortex samples compared to those from the PF cortex. Only the '*menopause*' input concept showed a greater association with the Pf cortex data.

Through ranking of the top 20 strongest correlating proteins, a prioritized key group of proteins for each DEP list was created. Using *Enrichr*-based interrogation of ligand-induced Gene Expression Omnibus (GEO) dataset alterations we identified significantly-overlapping GEO dataset terms correlating to these top 20 DEPs. Extracting and then displaying, via word frequency-dependent wordclouds (font size indicating the relative frequencies), the words comprising these GEO perturbagen datasets a strong estrogen-related function was evident (Fig. 4D). When these 20 proteins were then cross-interrogated with a functional disease database, *i.e.* the JENSEN Disease database (https://diseases.jensenlab.org/) a common signature of '*Neurodegenerative disease'* was seen for Rs and Pf datasets. In agreement with our previous pathway analysis the enrichment score (*Enrichr* 'Combined Score') for the Rs cortex tissues was nearly twice that for the Pf cortex, reinforcing our hypothesis that an estrogen-mediated dysfunction induces a strong pro-neurodegenerative effect on the Rs cortex with a milder effect seen in the Pf cortex.

DISCUSSION

Using the highly translational method of rsfMRI, we have demonstrated that endocrine disruption, by ovariectomy, prevented the strengthening of A-P connectivity between three and seven months. In contrast to Sham mice, OVX mice displayed low A-P connectivity throughout the ages examined. The increase of this long-range FC in Sham mice likely reflects further maturation of the intrinsic functional networks, in line with data showing that although gross structural changes have already occurred by

544 the age of three months in mice, minor alterations are still ongoing between three and six months of
545 age (Hammelrath et al., 2016). Interestingly, long-range connections typically develop only later in life,
546 towards adulthood (Dennis and Thompson, 2013; Fair et al., 2009), and have been previously
547 identified to be more vulnerable to aging effects due to a complex interplay between structural and
548 neurotransmission alterations as well as energy efficiency necessary to maintain these long-range
549 connections (Tomasi and Volkow, 2012). As evidenced by our quantitative proteomics analysis, the FC
550 pattern in OVX mice co-existed with an accelerated ageing molecular phenotype (Fig. 3A-C). This is
551 further supported by human studies (Levine et al., 2016; Rocca et al., 2016; Rocca et al., 2017) showing
552 that premature loss of gonadal hormones in women after bilateral ovariectomy is linked with signs of
553 accelerated aging (Rocca et al., 2017).
554
555 We confirmed the co-existence of aberrant A-P FC and cognitive deficits in adult OVX mice, reflected
556 by impaired memory retention in the Barnes maze and PA test. This is in agreement with human data
557 showing that the strength of A-P FC is related to cognitive performance in healthy aging adults and
558 patients with mild cognitive impairment (Liang et al., 2011; Vidal-Pineiro et al., 2014). As estrogen
559 receptors are present in, among others, the hippocampus and cortical regions (Pf cortex) (Hazell et
560 al., 2009; Mitra et al., 2003), these regions are highly targeted in OVX literature. In the present study
561 the earliest pathological signs were observed in cortical regions, *i.e.* the interaction between Pf and
562 Rs regions, which is in agreement with the fact that we did not observe hippocampal-dependent
563 learning deficits. In contrast to acquisition or memory formation, which involves hippocampal-cortical
564 communication, memory retention is mainly driven by the integration of cortical regions (Bontempi
565 et al., 1999; Izquierdo and Medina, 1997; Maviel et al., 2004; Miller, 2000; Todd and Bucci, 2015).
566 Additionally, the medial Pf cortex has been proposed to be involved in encoding fear learning (Herry
567 and Johansen, 2014) corroborating the impaired PA performance demonstrated in OVX mice.
568 Although the Pf cortex is also important for functions such as working memory (Shanmugan and
569 Epperson, 2014), we did not observe specific working memory deficits after OVX which is also

supported by the fact that no local FC change was present in this region. Additionally, working memory also relies on the integration of other brain areas, such as the hippocampus, perirhinal cortex, thalamus and basal forebrain (Dere et al., 2007; Lalonde, 2002), so it is possible that these regions can compensate for any Pf dysfunction.

Whereas memory deficits in this study are in line with the posit that OVX or menopause are linked with impaired cognitive function (Blair et al., 2016; Heikkinen et al., 2004; Iivonen et al., 2006), it is important to note that some discrepancies can be seen with respect to timing of OVX and duration of hormone depletion as well as the variety in cognitive function investigated (Bastos et al., 2015; Heikkinen et al., 2004). One limitation within this study might be that we only evaluated behavioral performance at the age of seven months, guided by the neuroimaging results. Therefore, no inference can be made as to which deficit occured first: functional or behavioral impairments. Nevertheless, it is noteworthy that functional changes were only detectable four months after ovariectomy, which is coincident with the so-called 'critical window' for estrogen replacement therapy (Blair et al., 2016). During this four month interval, many alterations might have occurred within the brain – as shown by our extensive proteomics analysis as well. As such, it can be argued that at this time point, the hormonal deprivation has led to irreversible changes to the neuronal system, including structural and neurotransmissive alterations. Therefore, functional connectivity alterations - and by extension also the behavioral changes – might also be driven by further downstream alterations in a cascade originally initiated by the OVX intervention.

Further investigation into the molecular signaling pattern underlying FC and cognitive changes indicated alterations of multiple proteins reflecting a neurodegenerative or neurodevelopmental pathology in the Rs and Pf cortex, respectively. The upregulation of pro-developmental and neuronal survival factors within the Pf region could be explained by the high level of resilience and neuroplasticity in this region throughout life (Kolb and Gibb, 2015). Reinforcement of these processes also supports the idea that OVX mice might demonstrate a compensatory mechanism to preserve the

596 local FC and prevent further deterioration. Nevertheless, despite these seemingly positive
597 reinforcement mechanisms, the DEP patterns from the Pf region were also strongly related with
598 estrogenic dysfunction, aging and neurodegeneration. Although molecular alterations in both regions
599 were clearly linked to hormonal and neurodegenerative processes, as shown by the NLP analysis, it
600 was obvious that the Rs cortex was most affected both by number and degree of textual correlation
601 to our specific '*concept*' terms. This perhaps suggests that the proteomic alterations here were most
602 profoundly affected, compared to the Pf cortex samples, by disruption to estrogenic functionality. This
603 also correlates to the more 'pathological' alteration of signaling pathways and also reproductive
604 signaling systems (*e.g*. the RXFP3 receptor) observed with our pathway analysis of Rs cortex samples
605 compared to those from the Pf cortex. Only the 'menopause' input concept showed a greater
606 association with the Pf cortex data. It is interesting to note that here we found an alteration in the
607 expression of Srd5a2 (3-oxo-5α-steroid 4-dehydrogenase 2, or 5-alpha reductase 2). This enzyme is
608 involved in the functional processing of androgens and thus its elevation in the Pf cortex region may
609 be indicative of an ameliorative response in this brain region to compensate the more pathological
610 signatures observed in the Rs cortex.
611
612 Although a clear distinct pattern was present in both regions, we also found a considerable proportion
613 of commonality between both regions. On the protein-level, both regions showed a significant
614 upregulation of rotatin (Rttn). This protein is implicated in early cortical development and mutations
615 of the Rttn gene can lead to microcephaly and polymicrogyria (Kheradmand Kia et al., 2012;
616 Shamseldin et al., 2015). However, it has never been described before in the adult brain. It is possible
617 that after the OVX intervention, neurons are forced to take on a more immature state due to the loss
618 of normal hormonal input signaling which might explain increased expression of such developmental
619 protein. Further research is required to unravel its role in the adult brain and its implication in the
620 hormonal regulation of brain structure and function.

According to the network-based deconvolution of the common DEP list, the axogenesis subnetwork was centered upon Nefl, an important neural cytoskeleton protein. An increase of Nefl has been previously linked to axonal damage and has thus been proposed as a promising marker for the progression of neurodegenerative disorders (Bacioglu et al., 2016). Beside these structural alterations, the driving force behind the observed FC and cognitive deficits was most likely altered dopaminergic function as this was found to be most significantly altered in both regions in the pathway and upstream regulator analyses. The link between the dopaminergic system, cognition and hormones is supported by several studies (Barth et al., 2015; Bosse and DiPaolo, 1996; Izquierdo and Medina, 1997; Jacobs and D'Esposito, 2011). Here, we found reduced FC coincident with upregulation of dopamine-related proteins after OVX. Indeed, it has been proposed that both insufficient and excessive levels of dopamine can lead to Pf dysfunction and cognitive deficits (Jacobs and D'Esposito, 2011). Further, a predicted common upstream regulator found in both regions was the dopamine receptor D3 (DRD3), which is implicated in synaptic plasticity and memory processes. This is in line with data showing that DRD3 knockout mice present improved cognitive function both after OVX (Cao et al., 2013) and upon aging (Xing et al., 2010). Moreover, antagonists for the DRD3 receptor have been proposed to benefit cognitive function and learning performance in rodents (Laszy et al., 2005). It is further interesting to note that for the Pf sample disease analysis a nerve conduction disorder was prominent in the output data, *i.e*. 'Canavan disease' [DOID:3613: https://diseases.jensenlab.org/]. This finding indicates that potential dysmyelination of the dopaminergic tracts between the Pf and Rs cortex may underpin the neurodegenerative effect induced by HPG dysfunction.

Finally, it is important to mention that the scope of our current study was to first examine whether resting state functional alterations occur after endocrine disruptions and, secondly, to evaluate the ability of neuroimage-guided molecular investigations to elucidate and help interpret complex molecular phenotypes. In this present study, however, we cannot discount that the endocrine disruptions observed, and not potential epigenetic, metabolic or vascular alterations, are solely the

cause of the DEP patterns observed in the two differing brain regions. These questions however remain an important potential new avenue for our continued research.

CONCLUSION

Within the present study, we have shown that ovariectomy in mice attenuates long-range anterior-posterior functional connectivity and leads to cognitive deficits at adult age. We identified that these functional and cognitive changes were driven by underlying pathological molecular signaling patterns, reflecting an imbalance between pro-neurodevelopmental and pro-neurodegenerative processes in the Pf and Rs cortex, respectively. The molecular phenotype further showed a strong involvement of changes in aging and reproductive signaling, as well as altered structural aspects (axogenesis, myelination) and dopaminergic neurotransmissive function. These findings support the proposed detrimental impact of endocrine disruption on brain function and cognition as well as the potential of using resting state FC as a translational noninvasive readout.

DISCLOSURE STATEMENT

The authors report no actual or potential conflict of interest.

ACKNOWLEDGEMENTS

We thank Jonathan Janssens (Translational Neurobiology Group, University of Antwerp-VIB) and Charlotte Vanacker (Inserm U1172, University of Lille) for their technical assistance. This research was supported by the European Union's Seventh Framework Program under grant agreement number 278850 (INMiND), the Fund for Scientific Research Flanders (FWO) (grant agreements G057615N and 12S4815N), the Stichting Alzheimer Onderzoek (SAO-FRA, grant agreement 13026), the interdisciplinary PhD grant BOF DOCPRO 2014 (granted to MV), by a KP-BOF 2015 from the University of Antwerp (granted to FK) and by the Agence Nationale de la Recherche (ANR GRAND, ANR-17-CE16-0015-01 to VP). The authors thank the behavioral exploration platform for rodent (Federation of Neurosciences, Univ Lille, France) and Dr. Charlotte Laloux for her advices on behavioral analysis. The

9.4T Bruker MR system was in part funded by the Flemish Impulse funding for heavy scientific equipment (42/FA010100/123) granted to Prof. Dr. Annemie Van der Linden.

REFERENCES

Albertson, A.J., Navratil, A., Mignot, M., Dufourny, L., Cherrington, B., Skinner, D.C., 2008. Immunoreactive GnRH type I receptors in the mouse and sheep brain. J Chem Neuroanat 35(4), 326-333.

Andrews-Hanna, J.R., Snyder, A.Z., Vincent, J.L., Lustig, C., Head, D., Raichle, M.E., Buckner, R.L., 2007. Disruption of large-scale brain systems in advanced aging. Neuron 56(5), 924-935.

Arevalo, M.A., Azcoitia, I., Garcia-Segura, L.M., 2015. The neuroprotective actions of oestradiol and oestrogen receptors. Nat Rev Neurosci 16(1), 17-29.

Bacioglu, M., Maia, L.F., Preische, O., Schelle, J., Apel, A., Kaeser, S.A., Schweighauser, M., Eninger, T., Lambert, M., Pilotto, A., Shimshek, D.R., Neumann, U., Kahle, P.J., Staufenbiel, M., Neumann, M., Maetzler, W., Kuhle, J., Jucker, M., 2016. Neurofilament Light Chain in Blood and CSF as Marker of Disease Progression in Mouse Models and in Neurodegenerative Diseases. Neuron 91(2), 494-496.

Barth, C., Villringer, A., Sacher, J., 2015. Sex hormones affect neurotransmitters and shape the adult female brain during hormonal transition periods. Front Neurosci 9, 37.

Bastos, C.P., Pereira, L.M., Ferreira-Vieira, T.H., Drumond, L.E., Massensini, A.R., Moraes, M.F., Pereira, G.S., 2015. Object recognition memory deficit and depressive-like behavior caused by chronic ovariectomy can be transitorialy recovered by the acute activation of hippocampal estrogen receptors. Psychoneuroendocrinology 57, 14-25.

Blair, J.A., McGee, H., Bhatta, S., Palm, R., Casadesus, G., 2015. Hypothalamic-pituitary-gonadal axis involvement in learning and memory and Alzheimer's disease: more than "just" estrogen. Front Endocrinol (Lausanne) 6, 45.

Blair, J.A., Palm, R., Chang, J., McGee, H., Zhu, X., Wang, X., Casadesus, G., 2016. Luteinizing hormone downregulation but not estrogen replacement improves ovariectomy-associated cognition and spine density loss independently of treatment onset timing. Horm Behav 78, 60-66.

Bontempi, B., Laurent-Demir, C., Destrade, C., Jaffard, R., 1999. Time-dependent reorganization of brain circuitry underlying long-term memory storage. Nature 400(6745), 671-675.

Bosse, R., DiPaolo, T., 1996. The modulation of brain dopamine and GABAA receptors by estradiol: a clue for CNS changes occurring at menopause. Cell Mol Neurobiol 16(2), 199-212.

Brann, D.W., Dhandapani, K., Wakade, C., Mahesh, V.B., Khan, M.M., 2007. Neurotrophic and neuroprotective actions of estrogen: basic mechanisms and clinical implications. Steroids 72(5), 381-405.

Cai, H., Chen, H., Yi, T., Daimon, C.M., Boyle, J.P., Peers, C., Maudsley, S., Martin, B., 2013. VennPlex--a novel Venn diagram program for comparing and visualizing datasets with differentially regulated datapoints. PLoS One 8(1), e53388.

Cao, F., Zhang, H., Meng, X., Feng, J., Li, T., Wei, S., Li, S., 2013. Ovariectomy-mediated impairment of spatial working memory, but not reference memory, is attenuated by the knockout of the dopamine D(3) receptor in female mice. Behav Brain Res 247, 27-33.

Cashion, A., Stanfill, A., Thomas, F., Xu, L., Sutter, T., Eason, J., Ensell, M., Homayouni, R., 2013. Expression levels of obesity-related genes are associated with weight change in kidney transplant recipients. PLoS One 8(3), e59962.

Chadwick, W., Martin, B., Chapter, M.C., Park, S.S., Wang, L., Daimon, C.M., Brenneman, R., Maudsley, S., 2012. GIT2 acts as a potential keystone protein in functional hypothalamic networks associated with age-related phenotypic changes in rats. PLoS One 7(5), e36975.

Chen, H., Martin, B., Daimon, C.M., Maudsley, S., 2013. Effective use of latent semantic indexing and computational linguistics in biological and biomedical applications. Front Physiol 4, 8.

Comasco, E., Sundstrom-Poromaa, I., 2015. Neuroimaging the Menstrual Cycle and Premenstrual Dysphoric Disorder. Curr Psychiatry Rep 17(10), 77.

Damoiseaux, J.S., Beckmann, C.F., Arigita, E.J., Barkhof, F., Scheltens, P., Stam, C.J., Smith, S.M., Rombouts, S.A., 2008. Reduced resting-state brain activity in the "default network" in normal aging. Cereb Cortex 18(8), 1856-1864.

Das, A., Dikshit, M., Srivastava, S.R., Srivastava, U.K., Nath, C., 2002. Effect of ovariectomy and estrogen supplementation on brain acetylcholinesterase activity and passive-avoidance learning in rats. Can J Physiol Pharmacol 80(9), 907-914.

De Bondt, T., Smeets, D., Pullens, P., Van Hecke, W., Jacquemyn, Y., Parizel, P.M., 2015. Stability of resting state networks in the female brain during hormonal changes and their relation to premenstrual symptoms. Brain Res 1624, 275-285.

Dennis, E.L., Thompson, P.M., 2013. Typical and atypical brain development: a review of neuroimaging studies. Dialogues Clin Neurosci 15(3), 359-384.

Dere, E., Huston, J.P., De Souza Silva, M.A., 2007. The pharmacology, neuroanatomy and neurogenetics of one-trial object recognition in rodents. Neurosci Biobehav Rev 31(5), 673-704.

Fair, D.A., Cohen, A.L., Power, J.D., Dosenbach, N.U., Church, J.A., Miezin, F.M., Schlaggar, B.L., Petersen, S.E., 2009. Functional brain networks develop from a "local to distributed" organization. PLoS Comput Biol 5(5), e1000381.

Fonseca, C.S., Gusmao, I.D., Raslan, A.C., Monteiro, B.M., Massensini, A.R., Moraes, M.F., Pereira, G.S., 2013. Object recognition memory and temporal lobe activation after delayed estrogen replacement therapy. Neurobiol Learn Mem 101, 19-25.
Franklin, K.B.J.P., G., 2007. The Mouse Brain in Stereotaxic Coordinates, 3 ed. Elsevier, Amsterdam.
Hammelrath, L., Skokic, S., Khmelinskii, A., Hess, A., van der Knaap, N., Staring, M., Lelieveldt, B.P.F., Wiedermann, D., Hoehn, M., 2016. Morphological maturation of the mouse brain: An in vivo MRI and histology investigation. Neuroimage 125, 144-152.
Hara, Y., Waters, E.M., McEwen, B.S., Morrison, J.H., 2015. Estrogen Effects on Cognitive and Synaptic Health Over the Lifecourse. Physiol Rev 95(3), 785-807.
Hazell, G.G., Yao, S.T., Roper, J.A., Prossnitz, E.R., O'Carroll, A.M., Lolait, S.J., 2009. Localisation of GPR30, a novel G protein-coupled oestrogen receptor, suggests multiple functions in rodent brain and peripheral tissues. J Endocrinol 202(2), 223-236.
Heikkinen, T., Puolivali, J., Tanila, H., 2004. Effects of long-term ovariectomy and estrogen treatment on maze learning in aged mice. Exp Gerontol 39(9), 1277-1283.
Henderson, V.W., 2014. Alzheimer's disease: review of hormone therapy trials and implications for treatment and prevention after menopause. J Steroid Biochem Mol Biol 142, 99-106.
Herry, C., Johansen, J.P., 2014. Encoding of fear learning and memory in distributed neuronal circuits. Nat Neurosci 17(12), 1644-1654.
Hjelmervik, H., Hausmann, M., Osnes, B., Westerhausen, R., Specht, K., 2014. Resting states are resting traits--an FMRI study of sex differences and menstrual cycle effects in resting state cognitive control networks. PLoS One 9(7), e103492.
Horstink, M.W., Strijks, E., Dluzen, D.E., 2003. Estrogen and Parkinson's disease. Adv Neurol 91, 107-114.
Huang, J., Bai, F., Yang, X., Chen, C., Bao, X., Zhang, Y., 2015. Identifying brain functional alterations in postmenopausal women with cognitive impairment. Maturitas 81(3), 371-376.
Hughes, R.N., 2004. The value of spontaneous alternation behavior (SAB) as a test of retention in pharmacological investigations of memory. Neurosci Biobehav Rev 28(5), 497-505.
Iivonen, S., Heikkinen, T., Puolivali, J., Helisalmi, S., Hiltunen, M., Soininen, H., Tanila, H., 2006. Effects of estradiol on spatial learning, hippocampal cytochrome P450 19, and estrogen alpha and beta mRNA levels in ovariectomized female mice. Neuroscience 137(4), 1143-1152.
Izquierdo, I., Medina, J.H., 1997. Memory formation: the sequence of biochemical events in the hippocampus and its connection to activity in other brain structures. Neurobiol Learn Mem 68(3), 285-316.
Jacobs, E., D'Esposito, M., 2011. Estrogen shapes dopamine-dependent cognitive processes: implications for women's health. J Neurosci 31(14), 5286-5293.
Jonckers, E., Van Audekerke, J., De Visscher, G., Van der Linden, A., Verhoye, M., 2011. Functional connectivity fMRI of the rodent brain: comparison of functional connectivity networks in rat and mouse. PLoS One 6(4), e18876.
Kheradmand Kia, S., Verbeek, E., Engelen, E., Schot, R., Poot, R.A., de Coo, I.F., Lequin, M.H., Poulton, C.J., Pourfarzad, F., Grosveld, F.G., Brehm, A., de Wit, M.C., Oegema, R., Dobyns, W.B., Verheijen, F.W., Mancini, G.M., 2012. RTTN mutations link primary cilia function to organization of the human cerebral cortex. American journal of human genetics 91(3), 533-540.
Koebele, S.V., Bimonte-Nelson, H.A., 2016. Modeling menopause: The utility of rodents in translational behavioral endocrinology research. Maturitas 87, 5-17.
Koebele, S.V., Bimonte-Nelson, H.A., 2017. The endocrine-brain-aging triad where many paths meet: female reproductive hormone changes at midlife and their influence on circuits important for learning and memory. Exp Gerontol 94, 14-23.
Kolb, B., Gibb, R., 2015. Plasticity in the prefrontal cortex of adult rats. Front Cell Neurosci 9, 15.
Lalonde, R., 2002. The neurobiological basis of spontaneous alternation. Neurosci Biobehav Rev 26(1), 91-104.
Langbeen, A., Ginneken, C.V., Fransen, E., Bosmans, E., Leroy, J., Bols, P.E.J., 2016. Morphometrical analysis of preantral follicular survival of VEGF-treated bovine ovarian cortex tissue following xenotransplantation in an immune deficient mouse model. Anim Reprod Sci 168, 73-85.
Laszy, J., Laszlovszky, I., Gyertyan, I., 2005. Dopamine D3 receptor antagonists improve the learning performance in memory-impaired rats. Psychopharmacology (Berl) 179(3), 567-575.
Leger, M., Quiedeville, A., Bouet, V., Haelewyn, B., Boulouard, M., Schumann-Bard, P., Freret, T., 2013. Object recognition test in mice. Nat Protoc 8(12), 2531-2537.
Levine, M.E., Lu, A.T., Chen, B.H., Hernandez, D.G., Singleton, A.B., Ferrucci, L., Bandinelli, S., Salfati, E., Manson, J.E., Quach, A., Kusters, C.D., Kuh, D., Wong, A., Teschendorff, A.E., Widschwendter, M., Ritz, B.R., Absher, D., Assimes, T.L., Horvath, S., 2016. Menopause accelerates biological aging. Proc Natl Acad Sci U S A 113(33), 9327-9332.
Li, R., Cui, J., Shen, Y., 2014. Brain sex matters: estrogen in cognition and Alzheimer's disease. Mol Cell Endocrinol 389(1-2), 13-21.
Liang, P., Wang, Z., Yang, Y., Jia, X., Li, K., 2011. Functional disconnection and compensation in mild cognitive impairment: evidence from DLPFC connectivity using resting-state fMRI. PLoS One 6(7), e22153.
Lisofsky, N., Martensson, J., Eckert, A., Lindenberger, U., Gallinat, J., Kuhn, S., 2015. Hippocampal volume and functional connectivity changes during the female menstrual cycle. Neuroimage 118, 154-162.
Lu, D., Cai, H., Park, S.S., Siddiqui, S., Premont, R.T., Schmalzigaug, R., Paramasivam, M., Seidman, M., Bodogai, I., Biragyn, A., Daimon, C.M., Martin, B., Maudsley, S., 2015. Nuclear GIT2 is an ATM substrate and promotes DNA repair. Mol Cell Biol 35(7), 1081-1096.

Marciniak, E., Faivre, E., Dutar, P., Alves Pires, C., Demeyer, D., Caillierez, R., Laloux, C., Buee, L., Blum, D., Humez, S., 2015. The Chemokine MIP-1alpha/CCL3 impairs mouse hippocampal synaptic transmission, plasticity and memory. Sci Rep 5, 15862.
Martin, B., Chadwick, W., Janssens, J., Premont, R.T., Schmalzigaug, R., Becker, K.G., Lehrmann, E., Wood, W.H., Zhang, Y., Siddiqui, S., Park, S.S., Cong, W.N., Daimon, C.M., Maudsley, S., 2015. GIT2 Acts as a Systems-Level Coordinator of Neurometabolic Activity and Pathophysiological Aging. Front Endocrinol (Lausanne) 6, 191.
Maudsley, S., Chadwick, W., Wang, L., Zhou, Y., Martin, B., Park, S.S., 2011. Bioinformatic approaches to metabolic pathways analysis. Methods Mol Biol 756, 99-130.
Maviel, T., Durkin, T.P., Menzaghi, F., Bontempi, B., 2004. Sites of neocortical reorganization critical for remote spatial memory. Science 305(5680), 96-99.
Messina, A., Langlet, F., Chachlaki, K., Roa, J., Rasika, S., Jouy, N., Gallet, S., Gaytan, F., Parkash, J., Tena-Sempere, M., Giacobini, P., Prevot, V., 2016. A microRNA switch regulates the rise in hypothalamic GnRH production before puberty. Nat Neurosci 19(6), 835-844.
Miller, E.K., 2000. The prefrontal cortex and cognitive control. Nat Rev Neurosci 1(1), 59-65.
Mitra, S.W., Hoskin, E., Yudkovitz, J., Pear, L., Wilkinson, H.A., Hayashi, S., Pfaff, D.W., Ogawa, S., Rohrer, S.P., Schaeffer, J.M., McEwen, B.S., Alves, S.E., 2003. Immunolocalization of estrogen receptor beta in the mouse brain: comparison with estrogen receptor alpha. Endocrinology 144(5), 2055-2067.
Montarolo, F., Perga, S., Martire, S., Navone, D.N., Marchet, A., Leotta, D., Bertolotto, A., 2016. Altered NR4A Subfamily Gene Expression Level in Peripheral Blood of Parkinson's and Alzheimer's Disease Patients. Neurotox Res 30(3), 338-344.
Parker, W.H., Jacoby, V., Shoupe, D., Rocca, W., 2009. Effect of bilateral oophorectomy on women's long-term health. Womens Health (Lond) 5(5), 565-576.
Peper, J.S., van den Heuvel, M.P., Mandl, R.C., Hulshoff Pol, H.E., van Honk, J., 2011. Sex steroids and connectivity in the human brain: a review of neuroimaging studies. Psychoneuroendocrinology 36(8), 1101-1113.
Ping, S.E., Trieu, J., Wlodek, M.E., Barrett, G.L., 2008. Effects of estrogen on basal forebrain cholinergic neurons and spatial learning. J Neurosci Res 86(7), 1588-1598.
Reuter, M.S., Krumbiegel, M., Schluter, G., Ekici, A.B., Reis, A., Zweier, C., 2017. Haploinsufficiency of NR4A2 is associated with a neurodevelopmental phenotype with prominent language impairment. Am J Med Genet A 173(8), 2231-2234.
Rocca, W.A., Bower, J.H., Maraganore, D.M., Ahlskog, J.E., Grossardt, B.R., de Andrade, M., Melton, L.J., 3rd, 2008a. Increased risk of parkinsonism in women who underwent oophorectomy before menopause. Neurology 70(3), 200-209.
Rocca, W.A., Gazzuola-Rocca, L., Smith, C.Y., Grossardt, B.R., Faubion, S.S., Shuster, L.T., Kirkland, J.L., Stewart, E.A., Miller, V.M., 2016. Accelerated Accumulation of Multimorbidity After Bilateral Oophorectomy: A Population-Based Cohort Study. Mayo Clin Proc 91(11), 1577-1589.
Rocca, W.A., Gazzuola Rocca, L., Smith, C.Y., Grossardt, B.R., Faubion, S.S., Shuster, L.T., Kirkland, J.L., Stewart, E.A., Miller, V.M., 2017. Bilateral Oophorectomy and Accelerated Aging: Cause or Effect? J Gerontol A Biol Sci Med Sci 72(9), 1213-1217.
Rocca, W.A., Grossardt, B.R., Geda, Y.E., Gostout, B.S., Bower, J.H., Maraganore, D.M., de Andrade, M., Melton, L.J., 3rd, 2008b. Long-term risk of depressive and anxiety symptoms after early bilateral oophorectomy. Menopause 15(6), 1050-1059.
Rocca, W.A., Grossardt, B.R., Shuster, L.T., 2011. Oophorectomy, menopause, estrogen treatment, and cognitive aging: clinical evidence for a window of opportunity. Brain Res 1379, 188-198.
Ryan, K.D., Schwartz, N.B., 1980. Changes in serum hormone levels associated with male-induced ovulation in group-housed adult female mice. Endocrinology 106(3), 959-966.
Sacher, J., Okon-Singer, H., Villringer, A., 2013. Evidence from neuroimaging for the role of the menstrual cycle in the interplay of emotion and cognition. Front Hum Neurosci 7, 374.
Sakaki, M., Mather, M., 2012. How reward and emotional stimuli induce different reactions across the menstrual cycle. Soc Personal Psychol Compass 6(1), 1-17.
Sandstrom, N.J., Williams, C.L., 2001. Memory retention is modulated by acute estradiol and progesterone replacement. Behav Neurosci 115(2), 384-393.
Sarkaki, A., Amani, R., Badavi, M., Safahani, M., Aligholi, H., 2008. Effect of ovariectomy on reference memory version of Morris water maze in young adult rats. Iran Biomed J 12(2), 123-128.
Shah, D., Blockx, I., Keliris, G.A., Kara, F., Jonckers, E., Verhoye, M., Van der Linden, A., 2016a. Cholinergic and serotonergic modulations differentially affect large-scale functional networks in the mouse brain. Brain Struct Funct 221(6), 3067-3079.
Shah, D., Deleye, S., Verhoye, M., Staelens, S., Van der Linden, A., 2016b. Resting-state functional MRI and [18F]-FDG PET demonstrate differences in neuronal activity between commonly used mouse strains. Neuroimage 125, 571-577.
Shah, D., Latif-Hernandez, A., De Strooper, B., Saito, T., Saido, T., Verhoye, M., D'Hooge, R., Van der Linden, A., 2018. Spatial reversal learning defect coincides with hypersynchronous telencephalic BOLD functional connectivity in APP(NL-F/NL-F) knock-in mice. Sci Rep 8(1), 6264.
Shah, D., Praet, J., Latif Hernandez, A., Hofling, C., Anckaerts, C., Bard, F., Morawski, M., Detrez, J.R., Prinsen, E., Villa, A., De Vos, W.H., Maggi, A., D'Hooge, R., Balschun, D., Rossner, S., Verhoye, M., Van der Linden, A., 2016c. Early pathologic amyloid induces hypersynchrony of BOLD resting-state networks in transgenic mice and provides an early therapeutic window before amyloid plaque deposition. Alzheimers Dement 12(9), 964-976.
Shamseldin, H., Alazami, A.M., Manning, M., Hashem, A., Caluseiu, O., Tabarki, B., Esplin, E., Schelley, S., Innes, A.M., Parboosingh, J.S., Lamont, R., Care4Rare Canada, C., Majewski, J., Bernier, F.P., Alkuraya, F.S., 2015. RTTN Mutations Cause Primary Microcephaly and Primordial Dwarfism in Humans. American journal of human genetics 97(6), 862-868.

Shanmugan, S., Epperson, C.N., 2014. Estrogen and the prefrontal cortex: towards a new understanding of estrogen's effects on executive functions in the menopause transition. Hum Brain Mapp 35(3), 847-865.
Shughrue, P.J., Lane, M.V., Merchenthaler, I., 1997. Comparative distribution of estrogen receptor-alpha and -beta mRNA in the rat central nervous system. J Comp Neurol 388(4), 507-525.
Siddiqui, S., Lustig, A., Carter, A., Sankar, M., Daimon, C.M., Premont, R.T., Etienne, H., van Gastel, J., Azmi, A., Janssens, J., Becker, K.G., Zhang, Y., Wood, W., Lehrmann, E., Martin, J.G., Martin, B., Taub, D.D., Maudsley, S., 2017. Genomic deletion of GIT2 induces a premature age-related thymic dysfunction and systemic immune system disruption. Aging (Albany NY) 9(3), 706-740.
Steyn, F.J., Wan, Y., Clarkson, J., Veldhuis, J.D., Herbison, A.E., Chen, C., 2013. Development of a methodology for and assessment of pulsatile luteinizing hormone secretion in juvenile and adult male mice. Endocrinology 154(12), 4939-4945.
Sundstrom Poromaa, I., Gingnell, M., 2014. Menstrual cycle influence on cognitive function and emotion processing-from a reproductive perspective. Front Neurosci 8, 380.
Sunyer, B., Patil, S., Höger, H., Lubec, G., 2007. Barnes maze, a useful task to assess spatial reference memory in the mice.
Todd, T.P., Bucci, D.J., 2015. Retrosplenial Cortex and Long-Term Memory: Molecules to Behavior. Neural plasticity 2015, 414173.
Toffoletto, S., Lanzenberger, R., Gingnell, M., Sundstrom-Poromaa, I., Comasco, E., 2014. Emotional and cognitive functional imaging of estrogen and progesterone effects in the female human brain: a systematic review. Psychoneuroendocrinology 50, 28-52.
Tomasi, D., Volkow, N.D., 2012. Aging and functional brain networks. Mol Psychiatry 17(5), 471, 549-458.
van den Heuvel, M.P., Hulshoff Pol, H.E., 2010. Exploring the brain network: a review on resting-state fMRI functional connectivity. Eur Neuropsychopharmacol 20(8), 519-534.
van Gastel, J., Janssens, J., Etienne, H., Azmi, A., Maudsley, S., 2016. The synergistic GIT2-RXFP3 system in the brain and its importance in age-related disorders. Frontiers in Aging Neuroscience.
Vargas, K.G., Milic, J., Zaciragic, A., Wen, K.X., Jaspers, L., Nano, J., Dhana, K., Bramer, W.M., Kraja, B., van Beeck, E., Ikram, M.A., Muka, T., Franco, O.H., 2016. The functions of estrogen receptor beta in the female brain: A systematic review. Maturitas 93, 41-57.
Vega, J.N., Zurkovsky, L., Albert, K., Melo, A., Boyd, B., Dumas, J., Woodward, N., McDonald, B.C., Saykin, A.J., Park, J.H., Naylor, M., Newhouse, P.A., 2016. Altered Brain Connectivity in Early Postmenopausal Women with Subjective Cognitive Impairment. Front Neurosci 10, 433.
Vidal-Pineiro, D., Valls-Pedret, C., Fernandez-Cabello, S., Arenaza-Urquijo, E.M., Sala-Llonch, R., Solana, E., Bargallo, N., Junque, C., Ros, E., Bartres-Faz, D., 2014. Decreased Default Mode Network connectivity correlates with age-associated structural and cognitive changes. Front Aging Neurosci 6, 256.
Vina, J., Lloret, A., 2010. Why women have more Alzheimer's disease than men: gender and mitochondrial toxicity of amyloid-beta peptide. J Alzheimers Dis 20 Suppl 2, S527-533.
Wang, L., Chadwick, W., Park, S.S., Zhou, Y., Silver, N., Martin, B., Maudsley, S., 2010. Gonadotropin-releasing hormone receptor system: modulatory role in aging and neurodegeneration. CNS Neurol Disord Drug Targets 9(5), 651-660.
Wen, S., Gotze, I.N., Mai, O., Schauer, C., Leinders-Zufall, T., Boehm, U., 2011. Genetic identification of GnRH receptor neurons: a new model for studying neural circuits underlying reproductive physiology in the mouse brain. Endocrinology 152(4), 1515-1526.
Whitten, W.K., 1956. Modification of the oestrous cycle of the mouse by external stimuli associated with the male. J Endocrinol 13(4), 399-404.
Xing, B., Meng, X., Wei, S., Li, S., 2010. Influence of dopamine D3 receptor knockout on age-related decline of spatial memory. Neurosci Lett 481(3), 149-153.
Zarate, S., Stevnsner, T., Gredilla, R., 2017. Role of Estrogen and Other Sex Hormones in Brain Aging. Neuroprotection and DNA Repair. Front Aging Neurosci 9, 430.
Zerbi, V., Grandjean, J., Rudin, M., Wenderoth, N., 2015. Mapping the mouse brain with rs-fMRI: An optimized pipeline for functional network identification. Neuroimage 123, 11-21.

FIGURES

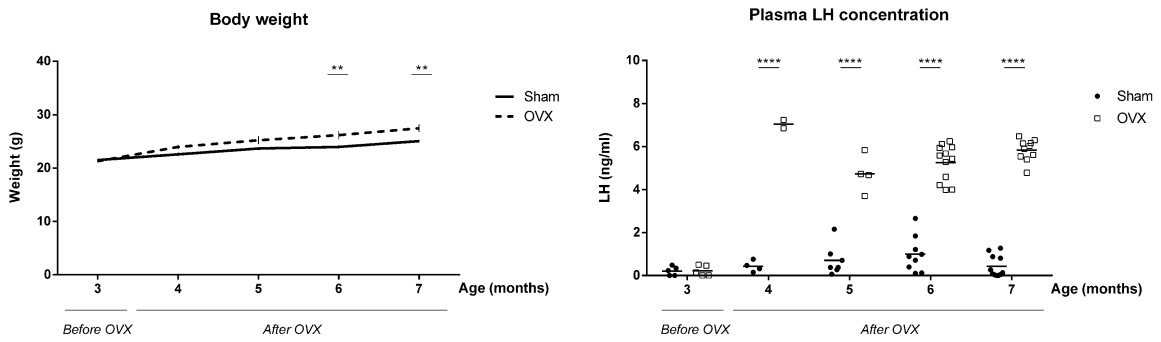

Figure 1. Body weight (A) and plasma luteinizing hormone (LH) concentration (B). A. Illustration of weight gain for both ovariectomized (OVX) and Sham groups over time. OVX mice had higher body weights compared to sham mice at 6 and 7 months of age. Results shown as mean ± SEM; individual values are indicated in light grey lines. **B.** Plasma LH concentration for both groups over time showing elevated plasma LH after OVX. ** $p<0.01$; **** $p<0.0001$. Results shown as mean overlaid on the individual values.

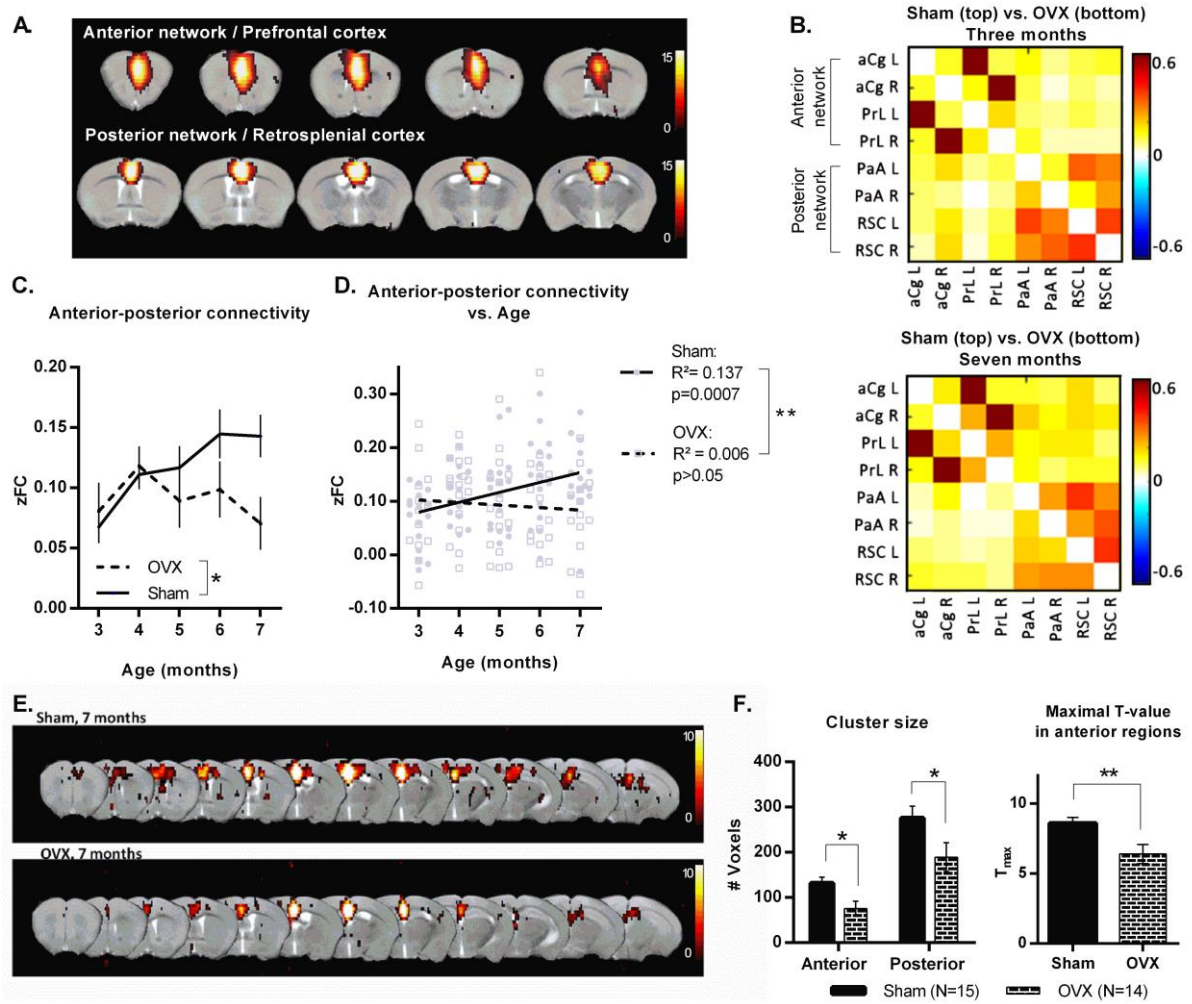

910
911 **Figure 2. Aberrant anterior-posterior functional connectivity (A-P FC) in ovariectomized mice**. **A.**
912 Illustration of relevant ICA components obtained from the group-level ICA of baseline rsfMRI data.
913 The colour scale represents t-values with yellow indicating a stronger correlation. **B.** Average zFC
914 matrices for three and seven month old Sham and OVX mice. Each square represents the correlation
915 between a pair of ROIs with the colour scale representing z-values. aCg: anterior cingulate cortex; PrL:
916 prelimbic cortex; PaA: parietal association cortex; RSC: retrosplenial cortex; L: left; R: Right. **C.** FC
917 between the anterior and posterior networks, based on matrices as illustrated in B. OVX mice have
918 consistently lower A-P FC compared to Shams.-**D**. Linear regression analysis between A-P FC and age
919 showing a significant positive correlation in the Sham group only. **E.** Group averaged statistical FC
920 maps obtained from a seed-based analysis at seven months with the Retrosplenial (Rs) cortex as seed.
921 Results are shown uncorrected, p<0.001, cluster size k>10, overlaid on an anatomical T_2-weighted
922 image. The colour scale indicates t-values with yellow representing a higher correlation with the seed

region. **F.** Cluster size (left graph) within the restrictions of the anterior and posterior network masks (A) for a seed in the Rs cortex (E). Maximal t-values (right graph) within the anterior network for a seed in the Rs cortex (E) confirms reduced A-P FC in OVX mice at 7 months. * $p<0.05$; ** $p<0.01$. Results shown as mean ± SEM.

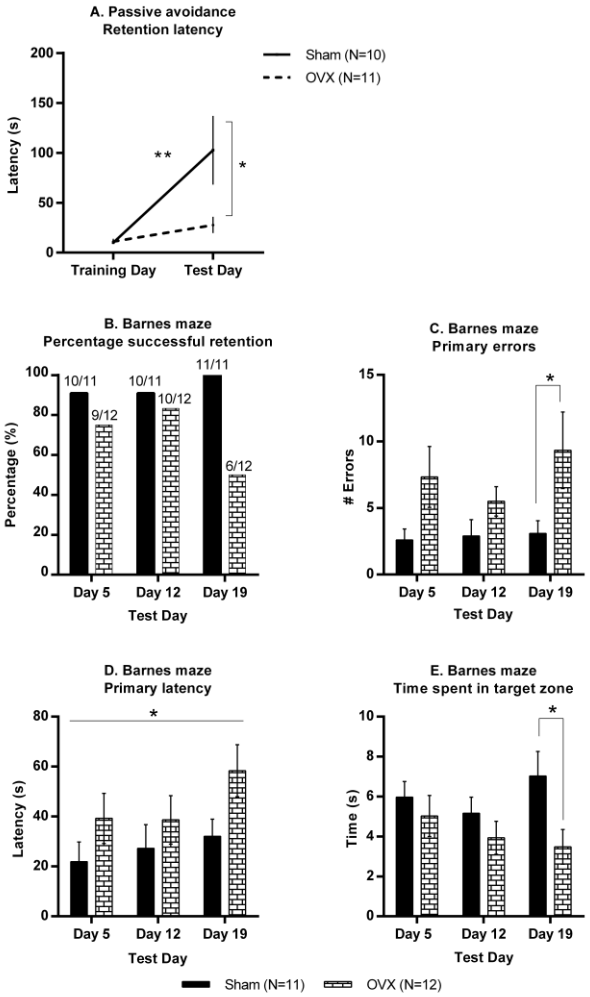

Figure 3. Cognitive impairments after four months of endocrine disruption. A. Retention latency for the passive avoidance (PA) test. OVX mice did not display increased latency on the test day, reflecting impaired PA retention ability. **B-E.** Barnes maze results. **B.** Percentage of mice per group that reached the target hole on each test day. Numbers above the bars indicate the actual number of mice reaching the target hole compared to the total group size. Only half of the OVX mice was able to locate the

target hole on day 19. **C.** Number of primary errors on the test days. OVX mice made significantly more primary errors compared to Sham mice, especially on day 19 . **D.** Primary latency across the test days. OVX mice performed less well than the sham mice ($p<0.05$), however no differences survived the multiple comparison correction. **E.** Time spent in the target zone on each test day. OVX mice spent considerably less time in the target hole compared to the sham group, an effect which was most pronounced on day 19. * $p<0.05$; ** $p<0.01$. Results shown as mean ± SEM.

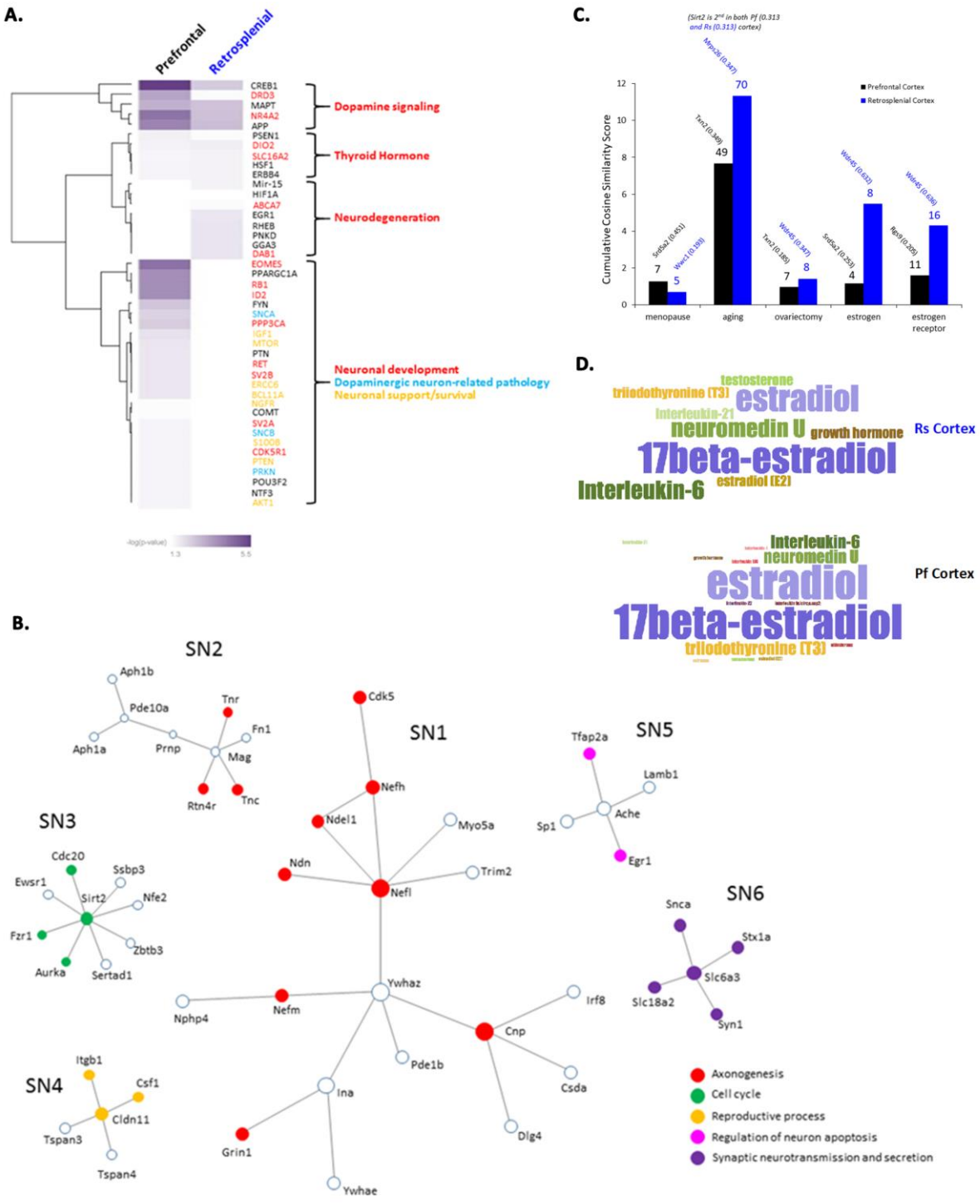

942

943 **Figure 4. Outcome of the quantitative proteomics. A.** IPA-based 'Upstream' functionality analysis.
944 Regulators associated with Dopamine-based signaling events were strongly linked to both cortex
945 tissues while potential upstream regulators linked to neurodegeneration/thyroid hormone signaling
946 were prominent in the retrosplenial cortex DEP patterns. DEP patterns from prefrontal cortical
947 samples from OVX mice were under the influence of more complex signaling activity, involving

potential regulators linked to neuronal development, generic neuronal support (yellow) or dopaminergic neuron pathology (turquoise). The associated key indicates the degree of pathway enrichment as a negative log10 of the primary probability value. **B.** Network-based deconvolution of the coherently-regulated protein signature common to prefrontal and retrosplenial cortex regions from OVX mice versus Sham mice. Six separate reliable subnetworks (SNs) were found – termed SN1 to SN6. The two most complex networks (SN1 and SN2) were most strongly associated with axogenesis (proteins mediating this GO term enrichment are highlighted as red circles- a similar representation is made in the subsequent subnetworks), while SN3 and SN4 were associated with Cell Cycle activity (green circles) and Reproductive Processed (orange circles) respectively. SNs 5 and 6 were both strongly associated with neurological functions, i.e. regulation of neuronal apoptosis (SN5 – pink circles) or synaptic neurotransmission (SN6 – purple circles). **C.** Targeted natural language processing (NLP). The graph shows the specific functional intersection between our user-defined 'concept' terms related to estrogenic activity in the brain and the DEP datasets from both cortical samples. For each protein-term score combination the number of proteins identified showing an implicit textual association with our user-defined concept is identified above the column. In addition, the highest Cosine Similarity-scoring protein from each sample against any of the specific concepts is indicated. **D.** Wordcloud showing a strong relation between our DEP profiles and estrogenic function. The significant overlap between the top 20 strongest correlating proteins (based on C) and GEO pertubagen datasets is presented as a word frequency-dependent wordcloud (font size indicating the relative frequencies).